Digital projection photochemical etching defines gray-scale features

Chris Edwards,[1] Kaiyuan Wang,[1] Renjie Zhou,[1] Basanta Bhaduri,[2] Gabriel Popescu,[2] and Lynford L. Goddard[1,*]

[1]*Micro and Nanotechnology Laboratory, Department of Electrical and Computer Engineering University of Illinois at Urbana-Champaign, Urbana, Illinois 61801, USA*

[2]*Quantitative Light Imaging Laboratory, Department of Electrical and Computer Engineering, Beckman Institute for Advanced Science and Technology, University of Illinois at Urbana-Champaign, Urbana, Illinois 61801, USA*

lgoddard@illinois.edu

Abstract: We demonstrate a maskless photochemical etching method that is capable of performing one-step etching of multi-level structures. This method uses a digital projector to focus an image onto the sample and define the etching pattern. By combining digital projection photochemical etching with diffraction phase microscopy, etch heights can be measured *in situ* in a non-destructive manner. This method is single shot, eliminating the need for expensive gray-scale masks or laser scanning methods. The etch rate is studied as a function of the wavelength and irradiance of the projected light. A lateral etch resolution of 2 μm is demonstrated by etching selected portions of the USAF-1951 target. Micropillars, multi-level plateaus, and an Archimedean spiral are etched, each in a single processing step, to illustrate the unique capabilities.

OCIS codes: (220.4610) Optical fabrication; (220.4000) Microstructure fabrication; (220.4241) Nanostructure fabrication; (220.3740) Lithography; (120.5050) Phase measurement.

References and links

1. G. Wysocki, J. Heitz, and D. Bauerle, "Near-field optical nanopatterning of crystalline silicon," Appl. Phys. Lett. **84**(12), 2025–2027 (2004).
2. Y. Jung, J. Kim, S. Jang, K. H. Baik, Y. G. Seo, and S.-M. Hwang, "Enhanced light extraction of nonpolar a-plane (11-20) GaN light emitting diodes on sapphire substrates by photo-enhanced chemical wet etching," Opt. Express **18**(9), 9728–9732 (2010).
3. T. D. Lowes and D. T. Cassidy, "Photochemical Etching of N-Inp as a Function of Temperature and Illumination," J. Appl. Phys. **68**(2), 814–819 (1990).
4. F. W. Ostermayer and P. A. Kohl, "Photoelectrochemical Etching of P-Gaas," J. Electrochem. Soc. **127**, C394–C394 (1980).
5. M. N. Ruberto, X. Zhang, R. Scarmozzino, A. E. Willner, D. V. Podlesnik, and R. M. Osgood, "The Laser-Controlled Micrometer-Scale Photoelectrochemical Etching of Iii-V Semiconductors," J. Electrochem. Soc. **138**(4), 1174–1185 (1991).
6. P. A. Kohl, "Photoelectrochemical etching of semiconductors," IBM J. Res. Develop. **42**(5), 629–638 (1998).
7. C. Youtsey, L. T. Romano, and I. Adesida, "Gallium nitride whiskers formed by selective photoenhanced wet etching of dislocations," Appl. Phys. Lett. **73**(6), 797–799 (1998).
8. X. M. Ding, Y. Kawaguchi, T. Sato, A. Narazaki, and H. Niino, "Fabrication of microarrays on fused silica plates using the laser-induced backside wet etching method," Langmuir **20**(22), 9769–9774 (2004).
9. S. Pissadakis, R. Böhme, and K. Zimmer, "Sub-micron periodic structuring of sapphire by laser induced backside wet etching technique," Opt. Express **15**(4), 1428–1433 (2007).
10. M. R. Wang and H. Su, "Laser direct-write gray-level mask and one-step etching for diffractive microlens fabrication," Appl. Opt. **37**(32), 7568–7576 (1998).
11. K. Sugioka, Y. Cheng, and K. Midorikawa, "Three-dimensional micromachining of glass using femtosecond laser for lab-on-a-chip device manufacture," Appl. Phys., A Mater. Sci. Process. **81**(1), 1–10 (2005).
12. F. Chen, H. W. Liu, Q. Yang, X. H. Wang, C. Hou, H. Bian, W. W. Liang, J. H. Si, and X. Hou, "Maskless fabrication of concave microlens arrays on silica glasses by a femtosecond-laser-enhanced local wet etching method," Opt. Express **18**(19), 20334–20343 (2010).
13. S. Ho, M. Haque, P. R. Herman, and J. S. Aitchison, "Femtosecond laser-assisted etching of three-dimensional inverted-woodpile structures in fused silica," Opt. Lett. **37**(10), 1682–1684 (2012).

#189146 - $15.00 USD Received 19 Apr 2013; revised 23 May 2013; accepted 23 May 2013; published 30 May 2013

14. K. Zimmer, R. Bohme, A. Braun, B. Rauschenbach, and F. Bigl, "Excimer laser-induced etching of sub-micron surface relief gratings in fused silica using phase grating projection," Appl. Phys., A Mater. Sci. Process. **74**(4), 453–456 (2002).
15. C. Vass, K. Osvay, and B. Hopp, "Fabrication of 150 nm period grating in fused silica by two-beam interferometric laser induced backside wet etching method," Opt. Express **14**(18), 8354–8359 (2006).
16. J. de Boor, N. Geyer, J. V. Wittemann, U. Gösele, and V. Schmidt, "Sub-100 nm silicon nanowires by laser interference lithography and metal-assisted etching," Nanotechnology **21**(9), 095302 (2010).
17. G. Popescu, *Quantitative Phase Imaging of Cells and Tissues*, Biophotonics (McGraw-Hill, New York, 2011).
18. G. Popescu, T. Ikeda, R. R. Dasari, and M. S. Feld, "Diffraction phase microscopy for quantifying cell structure and dynamics," Opt. Lett. **31**(6), 775–777 (2006).
19. C. Edwards, A. Arbabi, G. Popescu, and L. L. Goddard, "Optically monitoring and controlling nanoscale topography during semiconductor etching," Light Sci Appl **1**(9), e30 (2012).
20. R. Zhou, G. Popescu, and L. L. Goddard, "22 nm node wafer inspection using diffraction phase microscopy and image post-processing," SPIE **8681**, 8610G (2013).
21. R. Zhou, C. Edwards, A. Arbabi, G. Popescu, and L. L. Goddard, "Detecting 20 nm defects in large area nano-patterns using optical interferometric microscopy," submitted (2013).
22. E. Spyratou, I. Asproudis, D. Tsoutsi, C. Bacharis, K. Moutsouris, M. Makropoulou, and A. A. Serafetinides, "UV laser ablation of intraocular lenses: SEM and AFM microscopy examination of the biomaterial surface," Appl. Surf. Sci. **256**(8), 2539–2545 (2010).
23. S. J. Lim, W. Kim, and S. K. Shin, "Surface-Dependent, Ligand-Mediated Photochemical Etching of CdSe Nanoplatelets," J. Am. Chem. Soc. **134**(18), 7576–7579 (2012).
24. D. E. Aspnes and A. A. Studna, "Dielectric functions and optical parameters of Si, Ge, GaP, GaAs, GaSb, InP, InAs, and InSb from 1.5 to 6.0 eV," Phys. Rev. B **27**(2), 985–1009 (1983).
25. C. J. Hwang, "Optical Properties of N-Type GaAs. I. Determination of hole diffusion length from optical absorption and photoluminescence measurements," J. Appl. Phys. **40**(9), 3731–3739 (1969).
26. S. Gupta, M. Y. Frankel, J. A. Valdmanis, J. F. Whitaker, and G. A. Mourou, "Subpicosecond carrier lifetime in GaAs grown by molecular beam epitaxy at low temperatures," Appl. Phys. Rev. **59**, 3276–3278 (1991).

1. Introduction

Photochemical etching (PC etching) is a technique that can enable low-cost fabrication of semiconductor devices with grayscale topography. When light with sufficient energy is absorbed near the surface of a semiconductor material, minority carriers are generated that can then diffuse to the surface and act as a catalyst in the etching process. As a result, the etch rate for different materials in a given etching solution can be controlled by varying the irradiance and wavelength of the incident light.

Traditionally, photochemical [1–3] and photoelectrochemical [4–6] etching have been most often used to improve the material selectivity of particular etching steps within a fabrication process. Various structures have been fabricated using laser-assisted wet etching, which requires the aid of proximity masking in order to achieve competitive results [7–9]. For multi-level structures, gray-scale masks are used which allow varying amounts of light to pass through. However, these masks are very expensive and may require several iterative purchases as the process is perfected. As a consequence, focus has been shifted to direct writing techniques which use lasers as the etching tool, rather than gray-scale masks [10]. More complex structures can be created if laser scanning is used [11–13]. This serial laser writing technique requires precise scanning equipment and software control, and the throughput is relatively low. The interference of multiple laser beams has also been employed to bypass the diffraction limit and obtain sub-micron gratings [9, 14, 15] and nanostructures [16].

Quantitative phase imaging (QPI) is a rapidly emerging field which has found great success in the biomedical field [17]. QPI exploits the fact that the phase of the imaging field is often much more informative than the amplitude. The relative phase shift contains the desired topographical information about the sample under investigation [18]. Using QPI, we can accurately measure the etch rate while varying the wavelength and irradiance of the projected light. Here, we use a QPI technique called epi-illumination diffraction phase microscopy (epi-DPM) which utilizes a compact Mach-Zehnder interferometer in order to obtain the phase information and reconstruct the surface topography with nanometer accuracy [18–21]. This compact configuration is common-path which inherently cancels out most

#189146 - $15.00 USD Received 19 Apr 2013; revised 23 May 2013; accepted 23 May 2013; published 30 May 2013

mechanisms responsible for noise and is single-shot with acquisition speed limited only by the speed of the camera. This technique is also non-destructive and does not require staining or coating of the specimen. Recently, we built an epi-DPM system to operate in reflection and accommodate opaque samples [19–21].

Here we report a maskless photochemical etching instrument that combines our newly developed digital projection photochemical etching and epi-DPM methods [19]. Under this configuration, gray-scale color images from a digital projector are focused onto the sample's surface, eliminating the need for a physical mask. This allows for the fabrication of complex multi-level structures that are difficult to achieve using standard photolithography and etching. This technique possesses substantial potential for the fabrication of key electronic and photonic devices such as microlenses for light-emitting diodes (LEDs) and vertical-cavity surface-emitting lasers (VCSELs), vias for integrated circuits and microfluidic channels, tapered waveguides and complex interconnects. By integrating etching with the epi-DPM imaging system, we are able to measure the dimensions of the etched structures on site in a completely non-invasive manner which is not possible with scanning electron microscopy (SEM), transmission electron microscope (TEM) or other similar inspection methods [19, 22, 23].

2. Experimental setup

Figure 1 shows the experimental epi-DPM setup used for photochemical etching and imaging. The solid lines represent the light path for the PC etching and the dotted lines represent the light path for the epi-DPM imaging system, which are both part of the same setup. Details of the epi-DPM system can be found in [19]. Light from the projector propagates through the 3 lens system and is directed through the epi-train of an existing microscope (Z2 Axio Imager, Zeiss) via a beam splitter. The beam-splitter allows the laser beam used for epi-DPM imaging to also be fed into the back of the microscope. The system is aligned such that the image from the projector is focused in the sample plane.

Our configuration uses a 3 lens system with $f_0 = 7.5$ cm, $f_1 = 100$ cm, and $f_2 = 30$ cm. The distance between the first 2 lenses is $d_{01} = 17.5$ cm and the distance between the 2nd and 3rd lenses is $d_{12} = 160$ cm. These values were chosen in order to get the proper demagnification given our constraints. The first constraint being that the intermediate image focused in the field aperture plane of the microscope must be at least 30 cm away from the final lens since the lenses cannot be placed inside the microscope. The second constraint is that the first lens, having a 2" diameter, must be placed less than 10 cm away from the projector lens so that the entire projector beam passes through. The magnification from inside the projector to the object plane is $M_{p0} = 1.59$ and the magnification from the object plane to the conjugate field plane inside the microscope is $M_{12} = 0.25$. Given the microscope objective ($M_{obj} = 0.1$), the overall magnification from inside the projector to the sample plane is $M = 0.04$ which results in 3 pixels/μm in the sample plane. However, each pixel is blurred to a diffraction limited spot of 1.6 μm. We used multiple pixels per diffraction spot to achieve a smooth etch pattern without pixilation.

#189146 - $15.00 USD Received 19 Apr 2013; revised 23 May 2013; accepted 23 May 2013; published 30 May 2013

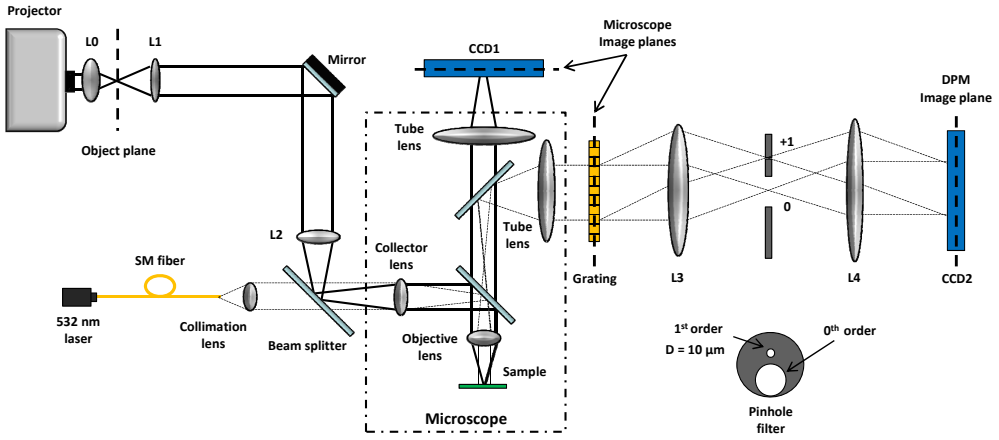

Fig. 1. Experimental epi-DPM setup used for photochemical etching and imaging. The thicker solid lines represent the light path from the projector, which was focused on the sample and aligned using CCD1. The epi-DPM system was used to measure the height of features on the sample using CCD2. The light path for epi-DPM is indicated with the thinner dotted lines.

All PC etching was done on n + GaAs wafers using 1:1:50 H_3PO_4:H_2O_2:H_2O as the etch solution. Here, hydrogen peroxide begins the process by oxidizing the GaAs and the phosphoric acid then removes the resulting oxide. Deionized water acts as the diluent and helps minimize the dark etch rate. The ratio of constituents has an effect on the etch rates, whether the solution is diffusion or reaction limited, and the surface roughness of etched features.

3. Experimental results

Before etching multi-layer structures, we first studied the etch rate for red, green, and blue light at different intensity levels using the epi-DPM system. Figure 2(a) shows the projected pattern used for determining the etch rates. This image was created in Microsoft PowerPoint using the standard eight bit red-green-blue (RGB) color scheme. Eight 30 µm squares which contain gray-levels of 32, 64, 96, 128, 160, 192, 224, and 255 were created for each color: red, green, and blue. To begin the etching procedure, 10 mL of 1:1:50 H_3PO_4:H_2O_2:H_2O was poured into a petri dish. The sample was placed into the petri dish containing the etchant and placed onto the microscope stage directly under the objective. A long working distance (16.1 mm) 10X, 0.2 NA objective was used for the etching. The sample was first brought into focus using the microscope and then the projected pattern was brought into focus by adjusting L_2 and observing it on CCD_1. Once the sample and projected image were both in focus, the light was turned up from 0.4% to 100% intensity. A 30 second etch was performed. The dark etch rate is 1.12 nm/s which results in minimal background etching. After the 30 seconds, the sample was cleaned using a standard degreasing. The sample was then imaged using epi-DPM on the same microscope with a 5X, 0.13 NA objective.

#189146 - $15.00 USD Received 19 Apr 2013; revised 23 May 2013; accepted 23 May 2013; published 30 May 2013

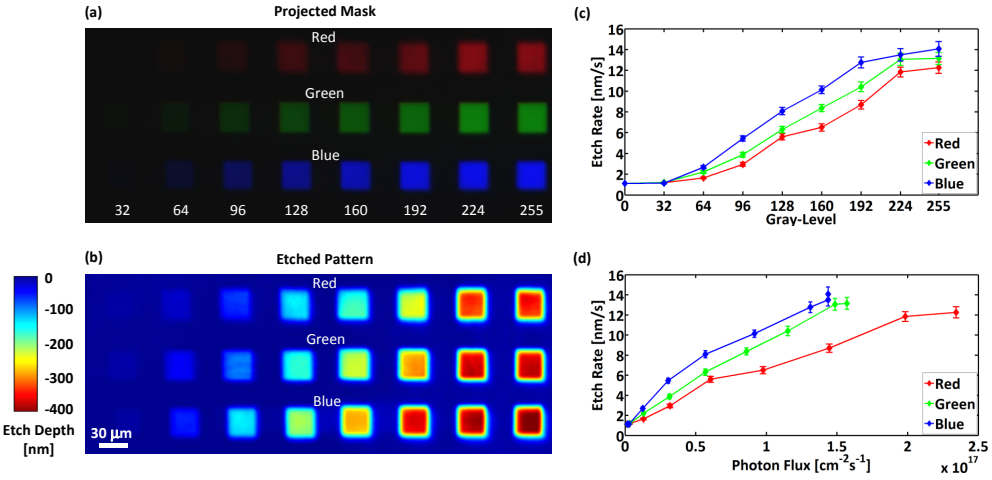

Fig. 2. Etch rate test. (a) Pattern focused onto sample plane. Eight squares of 32, 64, 96, 128, 160, 192, 224, and 255 were made of red, blue and green. A 30 second photochemical etch was performed using a solution of 1:1:50 H_3PO_4:H_2O_2:H_2O. (b) Etched squares corresponding to gray-levels indicated in (a). Etching was done using an LD 10X, 0.2 NA objective and imaging was done using a 5X, 0.13 NA objective via epi-DPM. (c) Absolute etch rates at each gray-level for each color. The background (dark) etch rate was 1.12 nm/s. (d) Etch rates versus photon flux for each color.

Figure 2(b) shows the etch depth of the squares measured with epi-DPM. The mean and standard deviation of the etch depth inside each square were recorded. The differential etch rates as a function of the gray-level for each color component were calculated using the recorded etch time and measured etch depths. Next, the background (dark) etch rate was measured. This allowed us to compute the absolute etch rate for the different colors and gray-levels as shown in Fig. 2(c). The error bars show the standard deviation. There is a small increase in roughness with increasing intensity of the projected light. The calculated absolute etch rates were used to compute the etch times required for a desired etch depth (or height) in subsequent etches. The power of the incident light was then measured in the sample plane using the Newport Optical Power Meter 1918-C. To better illustrate the photochemically induced etching on a per photon basis, the photon flux was computed by dividing the irradiance by the energy per photon. The etch rate versus photon flux is shown in Fig. 2(d). Here, we see a clear separation between the etch rates for the different colors. The bandgap of GaAs is E_g = 1.43 eV where the longest absorbing wavelength is λ_{max} = 868 nm. The absorption coefficient for GaAs is 3.93×10^4 cm^{-1}, 7.94×10^4 cm^{-1}, 1.24×10^5 cm^{-1} at 633 nm, 532 nm, and 488 nm respectively and the skin depth is 25.5 µm, 12.6 µm, 8.1 µm for these wavelengths [24]. In general, it is expected that the shorter wavelength light will result in higher etch rates (per photon) because carriers are created closer to the surface. The etching process is initially reaction-limited by the oxidation process. Incident light produces minority carriers (holes) that assist in the oxidation process. The etch rate begins to saturate at high intensities when the process becomes diffusion-limited. At this point, the local reagents are being consumed too quickly and the rate is slowed as new species must diffuse into the regions near the surface. To avoid saturation of the etchant and its adverse effects on etch quality, only gray-levels below 200 were used for subsequent etches.

To test the resolution of the photochemical etching process using our system, we created mask patterns using selected portions of the USAF-1951 target ranging from 16 µm down to 1.2 µm. The target contains features with sizes in discrete steps of 2.38 µm, 2 µm and 1.68 µm, which are close to our resolution limit. All colors resolve at 2.38 and 2 µm, but are not clearly resolved at 1.68 µm. The color green was used to illustrate our typical etch feature

#189146 - $15.00 USD Received 19 Apr 2013; revised 23 May 2013; accepted 23 May 2013; published 30 May 2013

resolution. In Fig. 3(a), the green portion was set to a grey-level of 96 and the background was set to 0. Low gray-levels were used for the resolution test, since higher intensities produce more roughness as seen in Fig. 2. This gives us a differential etch rate of 2.75 nm/s. A 36 second etch was performed following the procedure listed above. Figure 3(b) shows the etched sample imaged with a 5X, 0.13 NA objective resulting in a resolution of 2.5 μm and a field of view (FOV) of 250 x 335 μm^2. Figure 3(c) was taken with a 20X, 0.5 NA objective (650 nm resolution) and shows the collection of lines taken from the 1 series shown in the top-left corner of Fig. 3(b). A cross-section was taken along the horizontal lines (2 x 10 μm^2) showing that we are able to clearly resolve the 2 μm features from the resolution target. Note that 3 peaks are also faintly visible even at 1.4 μm. The etch feature resolution can be further reduced by using a higher NA long working distance objective. The etching resolution has three components: one from the diffraction limit of the light used in etching, one from the diffusion of carriers as a result of the photochemical etching process (about 1.1 μm for n + GaAs at room temperature [25]), and one from aberrations and imperfections in the optical system. The optical resolution limit for green light using the 10X, 0.2 LD objective is 1.6 μm according to Abbe's formula. Further broadening in the features is due to the diffusion of carriers and imperfections in the optical setup. Slight discrepancies between the vertical and horizontal resolution are most likely due to the rectangular geometry of the RGB subpixels inside the projector.

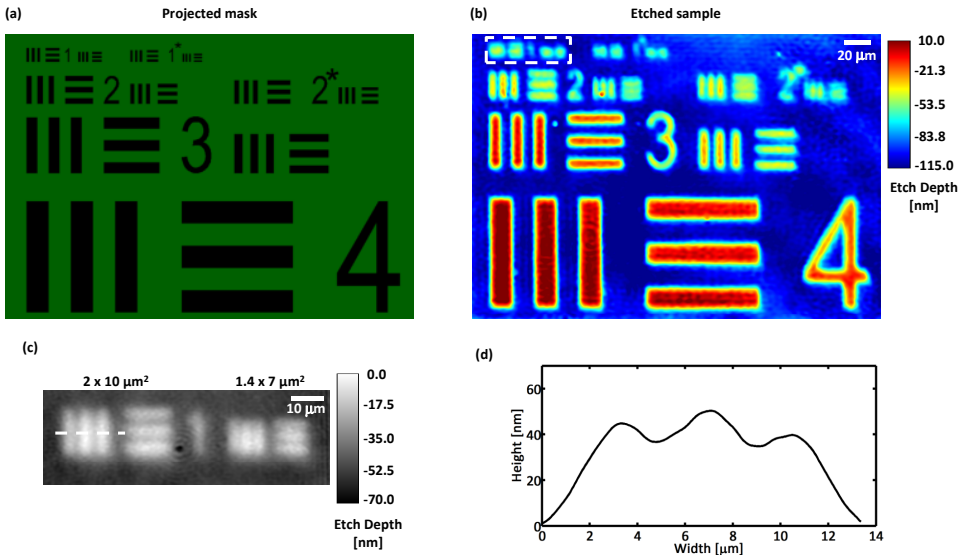

Fig. 3. Resolution Test. (a) Projector pattern (selected portions of the USAF-1951 target) focused onto the sample. (b) Etched sample imaged with 5X, 0.13 NA objective (2.5 μm lateral resolution). (c) Image from lines in series 1 captured using a 20X, NA = 0.5 objective (650 nm lateral resolution). (d) Cross-section of horizontal lines taken along dotted-line in (c). Based on this test, the lateral resolution of etched features using our photochemical etching setup is approximately 2 μm.

In Fig. 4, we show the topography images of different test structures fabricated with our system. Figure 4(a) is an image of our standard control sample, a micropillar, which was fabricated in a single 60 second etch. Since light itself is used to define the structure, there is no need for spinning and coating photoresist, aligning and exposing the sample, or developing. A projected image was used with grey-levels of 0 and 136 for the pillar and background respectively. PC etching was performed for 60 seconds resulting in a mean height of 304.9 nm. It was calibrated to have a 100 μm diameter and a height of 300 nm. Figure 4(b)

#189146 - $15.00 USD Received 19 Apr 2013; revised 23 May 2013; accepted 23 May 2013; published 30 May 2013

shows a cross-section of the pillar in (a) showing that the resulting width is 100 µm. A perfect isotropic wet etch using a photoresist mask results in 1 nm of undercutting per 1 nm of etching, resulting in an edge resolution of $\varepsilon = \Delta x/\Delta y = -1$. Here, we see a broadening effect instead of undercutting which is due to the diffusion of carriers and results in an edge

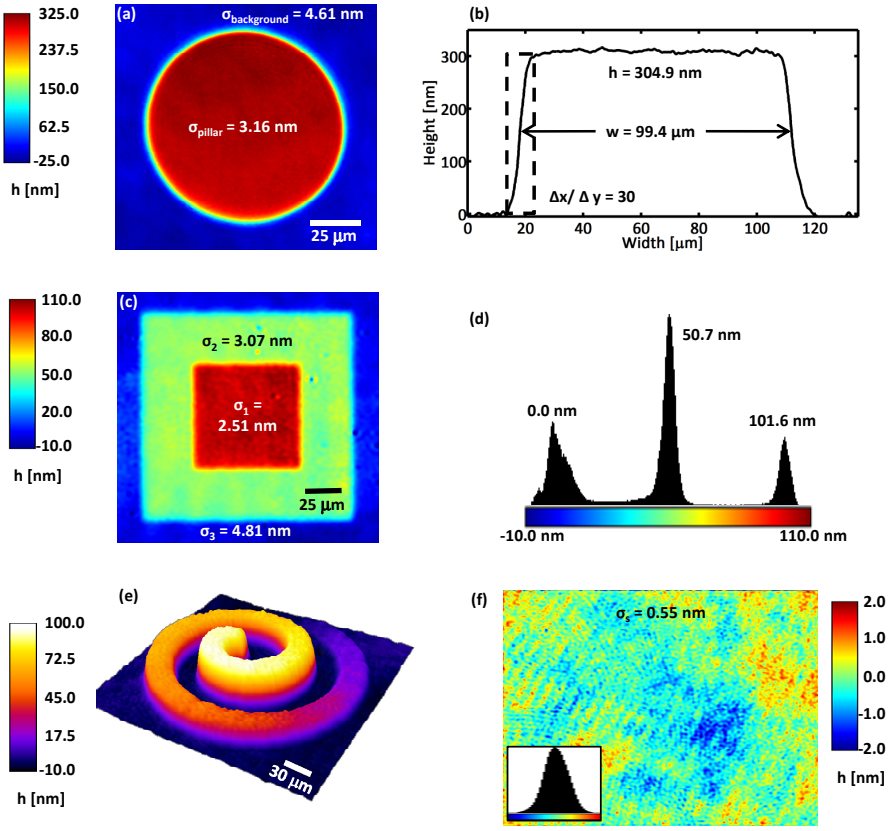

Fig. 4. Test structures. (a) DPM height map of a PC etched micropillar. A mask pattern with grey-levels of 0 and 136 was used for the pillar and background respectively. PC etching was performed for 60 seconds resulting in a mean height of 304.9 nm. (b) Cross-section of pillar in (a) showing the dimensions and edge resolution. (c) DPM height map of stacked plateaus. A projected image with grey-levels of 0, 60, and 78 were used for the mask pattern. Photochemical etching was performed for 33 seconds resulting in mean heights of 0, 50.7, and 101.6 nm. Histogram of image in (c) showing the heights of the three levels. (e) Topographical profile of PC etched Archimedean spiral. (f) DPM height image of a flat, unprocessed n + GaAs wafer. The standard deviation is used to quantify the spatial noise of the epi-DPM imaging system. The standard deviations of each layer in (a) and (c) were also measured. The roughness achieved using this method is comparable to that of standard wet etching.

resolution of $\varepsilon = \Delta x/\Delta y = 30$. This broadening effect is a major limitation of this new technique, but may be alleviated by pre-warping the projected pattern in order to achieve more vertical sidewalls. A sacrificial layer with a shorter carrier lifetime (i.e. diffusion length) [26] could also be used to pattern the desired gray-scale structure with sharper edges followed by an anisotropic dry etch to transfer the gray-scale pattern to the underlying layer. Figure 4(c) shows a topography image of multi-level plateaus also fabricated in a single etch step. A projected image with grey-levels of 0, 60, and 78 were used for the mask pattern. PC etching was performed for 33 seconds resulting in mean heights of 0, 50.7, and 101.6 nm. It was calibrated to have lateral dimensions of 150 µm and 75 µm with heights of 0 nm, 50 nm and 100 nm based on the etch rates computed in Fig. 2(c). Figure 4(d) shows a histogram of the

#189146 - $15.00 USD Received 19 Apr 2013; revised 23 May 2013; accepted 23 May 2013; published 30 May 2013

structure indicating the mean height of each of the three layers illustrating the excellent process control and repeatability. To further illustrate the strengths of the technique, we fabricated an Archimedean spiral using a continuous gray-scale image. The gray-level values decreased linearly around the spiral from 0 to 96. The maximum height and width were calibrated to be 100 nm and 30 μm respectively. Figure 4(e) shows the surface topography of an Archimedean spiral. This type of structure can only be etched using standard photolithographic techniques if the spiral is broken up into many discrete steps, each requiring a separate processing step. This structure was etched in 33 seconds. Figure 4(f) shows an epi-DPM image of a flat, unprocessed n + GaAs wafer. The mean height is zero but small height variations exist due to the presence of noise in the inspection instrument. Thus, the standard deviation of the height is a measure of the spatial noise and was measured to be 0.55 nm. In order to quantify the roughness of the etched structures, the standard deviations were also recorded for the various layers of each structure as reported in Figs. 4(a) and (c). These measurements show that the roughness is less than 5 nm for all cases, which is comparable to the roughness of a standard wet etch done under cleanroom conditions.

4. Conclusions

We have demonstrated an instrument that combines our newly developed digital projection photochemical etching and epi-DPM techniques. This method is capable of fabricating gray-scale structures that are otherwise difficult to obtain using standard photolithography. This method is also capable of etching multiple-step features in a single processing step. The etch rates were determined by varying the wavelength and irradiance of the projected light and used to calibrate the process. The projected images were calibrated to give the correct lateral dimensions and are accurate to within our 2 μm lateral etch feature resolution. The edge resolution of the etched structures was determined to be the major bottleneck, but may be alleviated by pre-warping the projected pattern. The roughness of etched features using this technique was also measured and is similar to that of standard wet etching. The dimensions of the etched samples were measured on site in a completely non-destructive manner using epi-DPM. A variety of structures with discrete or continuously varying heights were fabricated to illustrate the unique capabilities and characterize the limitations of this budding technology.

Acknowledgments

This work is supported in part by NSF CBET-1040462 MRI award with matching funds from the University of Illinois.

#189146 - $15.00 USD Received 19 Apr 2013; revised 23 May 2013; accepted 23 May 2013; published 30 May 2013